Eur. J. Biochem. 247, 545–557 (1997)

The solution structure and activity of caerin 1.1, an antimicrobial peptide from the Australian green tree frog, *Litoria splendida*

Herbert WONG[1], John H. BOWIE[2] and John A. CARVER[3]

[1] Industrial Research Limited, Lower Hutt, New Zealand
[2] Department of Chemistry, University of Adelaide, Australia
[3] Department of Chemistry, University of Wollongong, Australia

(Received 2 May 1997) – EJB 97 0634/3

Caerin 1.1 is one of the major antimicrobial peptides isolated from the skin of the Australian green tree frog, *Litoria splendida*. Two-dimensional ^{1}H-^{1}H and ^{1}H-^{13}C NMR spectroscopy in trifluoroethanol/H_2O (50:50, by vol.) have been used to assign the ^{1}H and ^{13}C-NMR spectra of this 25-amino-acid peptide. From an examination of these data, and using distance geometry and molecular dynamics calculations, the solution conformation of caerin 1.1 has been determined. The peptide adopts two well-defined helices from Leu2 to Lys11 and from Val17 to His24 separated by a region of less-defined helicity and greater flexibility. Overall, the peptide has a distinct amphipathic charge distribution. The solution structure of caerin 1.1 is compared with activity data against a variety of micro-organisms for the parent peptide and some naturally occurring and synthetic variants of caerin 1.1. The structural and activity data are consistent with caerin 1.1 interacting with membranes in a similar manner to other antimicrobial peptides, i.e. via a carpet-like mechanism whereby the individual peptides aggregate in a helical manner and orient themselves parallel to the membrane in a sheet-like arrangement [Shai, Y. (1995) *Trends Biochem. Sci.* 20, 460–464].

Keywords: antimicrobial peptide; NMR; solution structure; amphipathic helix.

The skins of amphibians are characterised by a rich variety of peptides (toxins and antibiotics) that form an integral part of the animal's defence system and regulate dermal physiological functions (Erspamer, 1994). In response to a variety of stimuli, the peptides are secreted from specialised granular glands located on the dorsal surface. Families of these types of peptides have been identified from a variety of frogs, e.g. the bombinins, brevinins and magainins (Bevins and Zasloff, 1990; Erspamer, 1994; Barra and Simmaco, 1995) and some have attracted pharmaceutical interest because of their antibiotic activity, e.g. a 22-amino-acid magainin analogue is currently undergoing clinical trials as a topical agent for treatment of impetigo (Jacob and Zasloff, 1994).

All antibiotic amphibian peptides are believed to function via a similar mechanism. Interaction occurs at the membrane surface with the peptide adopting an α-helical conformation which disrupts normal membrane function and leads to lysis of the bacterial cell wall. The magainin peptides (from the skin of the frog, *Xenopus laevis*) are the best studied of these peptides and solution- and solid-state NMR spectroscopic studies have shown that the peptides are unstructured in water but assume an amphipathic α-helical conformation in trifluoroethanol/water mixtures or when incorporated into artificial lipid bilayers (Marion et al., 1988; Bechinger et al., 1993). Magainin is positively charged and interacts readily with anionic phospholipids but will not lyse red blood cells or lymphocytes (Jacob and Zasloff, 1994). It has been proposed that this selectivity arises from red blood cells and lymphocytes having a low concentration of anionic phospholipids compared to bacterial cells.

Recently, the dermal secretions of Australian green tree frogs (*Litoria splendida*, *L. caerulea*, *L. xanthomera* and *L. gilleni*) have been examined and some 30 peptides have been isolated and their amino acid sequences elucidated (Stone et al., 1992a,b, 1993; Waugh et al., 1993, 1995; Steinborner et al., 1997). The major components from these frogs are caerulein and the caerin and caeridin families of peptides. Caerulein may have an hormonal role, the caerin peptides have antimicrobial activity whilst the caeridin peptides possess little antimicrobial activity and their function is unknown. Like magainin and other antibiotic peptides, the caerin peptides display a distinct amphipathic α-helical distribution of amino acids when placed on an Edmundsen helical wheel (Stone et al., 1992b; Steinborner et al., 1997) which is consistent with the postulate that all these peptides interact with membranes in a helical conformation. In this study, we have used NMR spectroscopy and computer-based molecular modelling techniques to determine the solution-state structure of caerin 1.1, the major caerin peptide from *Litoria splendida*. Caerin 1.1 is 25 amino acids in length and has the sequence:

GLLSV^{5}LGSVA^{10}KHVLP^{15}HVVPV^{20}IAEHL^{25}-NH_2.

In addition to caerin 1.1, eight other variants of caerin 1.1 have been isolated from *Litoria* species (Stone et al., 1992b,

Correspondence to J. A. Carver, Department of Chemistry, The University of Wollongong, Northfields Avenue, Wollongong, NSW 2522, Australia

Fax: +61 42 214 287.

Abbreviations. DQF COSY, double-quantum-filtered correlation spectroscopy; HSQC, heteronuclear single-quantum coherence; MIC, minimum inhibitory concentration; RMD, restrained molecular dynamics; 1D and 2D, one- and two-dimensional.

Table 1. Comparison of the antimicrobial activities of caerin 1.1 and some of its synthetic and naturally occurring (caerin 1.3) variants. Peptide 1.1D refers to the all-D-amino acid version of caerin 1.1; 1.1GP, 1.1PG, 1.1GG are synthetic, non-native caerin 1.1 variants with amino acid substitutions at the underlined positions; caerin 1.3 is naturally occurring. Sequences are as follows: 1.1, GLLSVLGSVAKHVLPHVVPVIAEHL; 1.1D, GLLSVLGSVAKHVLPHVVPVIAEHL; 1.1GP, GLLSVLGSVAKHVLGHVVPVIAEHL; 1.1PG, GLLSVLGSVAKHVLPHVVGVIAEHL; 1.1GG, GLLSVLGSVAKHVLGHVVGVIAEHL; 1.3, GLLSVLGSVAQHVLPHVVPVIAEHL; Caerin 1.1 has also been tested against HIV 1 (20), *Leuconostoc mesenteroides* (12.5), *Pasteurella haemolytica* (25), *Pseudomonas aeruginosa* (12.5), and *Streptococcus faecilis* (25). For *S. aureus*, the results are dependent upon the strain used.

Organism	MIC of peptide					
	1.1	1.1D	1.1GP	1.1PG	1.1GG	1.3
	μg/ml					
Bacillus cereus	50	50	100	100	50	50
Escherichia coli	>100	>100	>100	>100	>100	100
Leuconostoc lactis	1.5	3	12.5	12.5	12.5	25
Listeria innocua	25	50	50	25	50	100
Micrococcus luteus	12.5	6	25	12.5	12.5	1.5
Pasteurella multocida	25	25	50	50	100	25
Staphylococcus aureus	3–12	6–12	25–50	25	25–50	100
Staphylococcus epidermis	12.5	12.5	100	100	100	100
Streptococcus uberis	12.5	25	50	25	12.5	100

1993; Waugh et al., 1993; Steinborner et al., 1997). Some of these peptides (e.g. caerin 1.1.1 and 1.1.4) have two amino acids deleted from their N- and C-termini and are inactive (unpublished results). The remaining peptides are all 25 amino acids in length with minor amino acid substitutions, and all have variation in their activities toward different microorganisms (unpublished results).

The NMR studies were undertaken in trifluoroethanol/water mixtures under conditions which favoured the maximum amount of overall structure for the peptide. Trifluoroethanol is a solvent which enhances intra-molecular hydrogen bonding interactions but does not induce structure in regions which have no structural tendency (Sönnichsen et al., 1992). The overall goal of this study was to obtain insights into the mechanism of action of caerin 1.1, in particular its structure when interacting with membranes. Unlike magainin, caerin 1.1 contains two proline residues which are well known as helix-breaking residues (Richardson and Richardson, 1988; Presta and Rose, 1988). It was therefore of interest to ascertain the effect of these two residues on the helical propensity of caerin 1.1. The activity of caerin 1.1 and some of its naturally occurring and synthetic variants against various micro-organisms was also determined and the results were compared with the NMR-derived structure of caerin 1.1. From such a comparison, it is shown that the structural and activity data are highly complementary.

EXPERIMENTAL PROCEDURES

Preparation of synthetic caerin 1 peptides. Caerin 1 peptides were synthesised commercially (by Chiron Mimotopes) using L-amino acids via the standard Fmoc method (full details including protecting groups and deprotection have been reported recently by Maeji et al., 1995). Synthetic caerin 1.1 was shown to be identical with natural caerin 1.1 by FAB mass spectrometry, Edman sequencing, and co-elution of the synthetic and natural peptides on HPLC.

Antimicrobial testing. The synthetic peptides were tested by Dr B. Winter (Microbiology Department of the Institute of Medical and Veterinary Science, Adelaide). The method used involved the measurement of inhibition zones (produced by the applied peptide) on a thin agarose plate containing the micro-organisms under study. The procedures are standard and have been fully documented (Jorgensen et al., 1993). Activities were recorded as MIC values, i.e. the minimum inhibitory concentration of peptide required to inhibit totally the growth of the particular micro-organism.

Circular dichroic spectroscopy. CD spectra were acquired on a Jobin-Yvon CD-6 spectrophotometer at room temperature. CD spectra of caerin 1.1 were acquired at a concentration of 27 μM, pH 4.7 in H_2O and concentrations of trifluoroethanol from 0 to 50% (by vol.). The pathlength was 1 mm and each spectrum represented an average of five scans.

NMR spectrosopy. For NMR studies, 8.5 mg caerin 1.1 was dissolved in 0.6 ml H_2O/($^2H_2$)trifluoroethanol (1:1, by vol.) at a pH meter reading of 2.7 to give a final concentration of 5.5 mM. ^{1}H-NMR spectra were acquired at 400 MHz on a Varian Unity-400 spectrometer and at 600 MHz on a Bruker DMX-600 spectrometer. ^{13}C-NMR spectra were acquired at 150.9 MHz on the latter spectrometer; for spectra acquired on this spectrometer, digital sampling was employed. The CH_2 resonance of trifluoroethanol was used as a chemical shift resonance in the ^{1}H-NMR (3.918 ppm) and ^{13}C-NMR (60.975 ppm) experiments.

All two-dimensional (2D) data sets used for assignment and structure generation were acquired at 25 °C. For spectra acquired at this and higher temperatures, probe temperature was calibrated using ethylene glycol. Double-quantum-filtered correlation spectroscopy (DQF-COSY; Rance et al., 1983), total correlation spectroscopy (TOCSY; Davis and Bax, 1985) and nuclear Overhauser effect spectroscopy (NOESY; Jeener et al., 1979) were all collected in the phase-sensitive mode using time proportional phase incrementation (Marion and Wüthrich, 1983) in t_1. For each experiment, 32 scans were time averaged for each of the 512 t_1 increments. Each complex free induction decay in t_2 consisted of 2048 complex data points over a spectral width of 5521.8 Hz. The transmitter frequency was centred on the water resonance and conventional low power presaturation from the same frequency synthesizer applied during a 1.5-s relaxation delay was used to suppress the large water signal in the TOCSY and NOESY spectra. Gradient methods for water suppression were employed in the DQF-COSY spectrum (John et al., 1992). TOCSY spectra were acquired with the pulse sequence of Griesinger et al. (1988), i.e. the clean-TOCSY experiment to minimise cross relaxation effects, using an MLEV-17 pulse train for

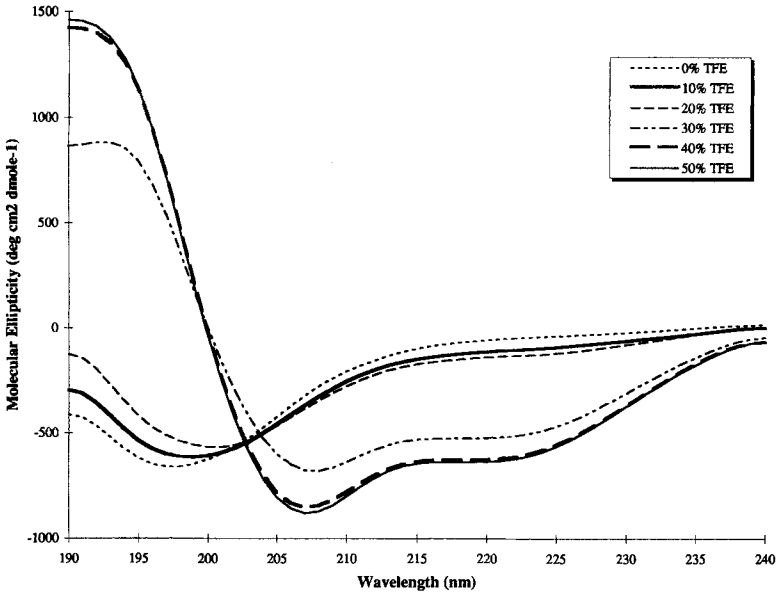

Fig. 1. CD spectra of caerin 1.1 at the varying concentrations (by vol.) of trifluoroethanol (TFE) indicated.

the spin lock mixing time. Two experiments were acquired with mixing times of 27.2 and 66.9 ms. NOESY spectra were collected with mixing times of 80, 150 and 250 ms. A heteronuclear single-quantum coherence (HSQC; Kay et al., 1992) experiment was acquired to assign the protonated ^{13}C resonances of caerin 1.1 via correlations to their attached protons. For this experiment, 512 t_1 increments were acquired over 4096 data points and 5521.8 Hz in the directly detected (^1H, F_2) dimension with a sweep width in the ^{13}C (F_1) dimension of 24146.5 Hz.

All 2D NMR spectra were processed on a Silicon Graphics Indy workstation using Felix 95 software from Molecular Simulations Inc. (MSI). Data matrices were multiplied by a 70−80° shifted sine-squared bell function in both dimensions. For the ^1H-NMR experiments, this weighting function was applied over 1024 data points in t_2 before zero filling to 2048 real data points and Fourier transformation. For the DQF-COSY and NOESY spectra, the weighting function in t_1 was applied to 512 real data points before zero filling to 2048 real points and Fourier transformation. For the TOCSY spectra, the weighting function was applied over 1024 points. The HSQC spectrum was zero-filled only in t_1 with the weighting functions being applied over 2048 data points in t_2 and 512 data points in t_1. All final, processed 2D NMR matrices consisted of 2048×2048 real points.

Structure generation. The NMRchitect (MSI) NMR structure refinement package was used to generate solution structures of caerin 1.1. The software incorporates Havel's DGII distance geometry program (Havel, 1991) to generate a family of structures followed by dynamical simulated annealing or restrained molecular dynamics (RMD) calculations to lower the overall energy of the structures. The NOESY spectrum of mixing time = 150 ms was used to generate distances for input into these calculations. On the basis of the strength of the isolated NOE cross-peak between the γ-CH_2 and δ-CH_2 groups of Pro15 (a fixed distance of 0.23 nm), NOEs were classified into three groups with strong, medium and weak intensities corresponding to distance bounds of 0.18−0.25 nm, 0.18−0.35 nm and 0.18−0.50 nm, respectively. All calculations were performed on the Indy workstation. Where appropriate (e.g. to take account of non-stereospecifically assigned protons), pseudo-atom corrections were applied to the distances (Wüthrich et al., 1983). Valine γ-CH_3 resonances were stereospecifically assigned using the method of Zuiderweg et al. (1985). From analysis of the NOESY spectra, 238 distance restraints were obtained after selecting the weaker of a symmetric pair of cross peaks and discarding any cross peaks that overlapped by more than 15%. After pseudo-atom corrections, these distance restraints comprised 138 intra-residue restraints, 59 restraints between adjacent (i,i+1) residues, seven restraints between residues two distant in the polypeptide chain (i,i+2), 28 restraints for protons three residues apart (i,i+3) and six restraints for protons four residues apart (i,i+4).

The quality of structures after embedding and during RMD was measured via an error function which consisted of a weighted linear combination of three generalised terms involving the magnitude of violations of the following restraints: (a) hard sphere lower-bound restraints (Van der Waals contacts), (b) the remaining lower and upper-bound (which includes the NOE distance) restraints and (c) the chirality restraints. Relative to the upper-bound restraints, the weighting factors for the remaining distance and chirality restraints were 0.2 and 0.1, respectively. It might appear that relatively greater emphasis was placed on achieving compliance with upper-bound restraints; however, from the results for structures 2 and 7 (see below), violations of lower-bound distance restraints can make a relatively large contribution to the error function.

For structure calculations, the parameter values chosen were mainly the MSI recommended default ones except that group tetrangle smoothing was used between all pairs of residues, metrisation was prospective, initial starting energy was set to 2090 kJ mol^{-1}, a penalty NOE lower and upper-bound distance force constant of 1.254 kJ · mol^{-1} · nm^{-2} was used and failure level, which determines whether the alternative chirality conformer is refined, was set to an error function value of 2.2. Tetrangle bounds smoothing of constraints was uneventful except that 49 of the 238 input NOE distance restraints were automatically replaced by tighter intra-residue covalent restraints. The RMD approach implemented in NMRchitect is relatively mild with annealing temperatures being limited to around 200 K. Following RMD, structures with error functions less than the failure level were minimised with respect to potential energy via steepest-descent or conjugate-gradient methods. The final run produced 20 conformers from which the first 10 conformers were arbitrarily chosen for examination.

Table 2. ^{1}H and ^{13}C-NMR chemical shifts for caerin 1.1 in trifluoroethanol/H_2O (1:1, by vol.) pH 2.7, 25°C. Assignments for all the ^{1}H-NMR resonances are presented whereas only the ^{13}C α-CH resonances are tabulated; n.o., not observed.

Residue	Chemical shift of				
	NH	α-CH	β-CH	others	α-^{13}CH
	ppm				
Gly1	n.o.	3.87, 4.04			42.2
Leu2	8.61	4.16	1.68	γ-CH 1.67 δ-CH_3 0.94, 0.98	57.0
Leu3	8.21	4.17	1.77	γ-CH 1.64 δ-CH_3 0.91, 0.91	57.0
Ser4	7.85	4.31	4.03		60.3
Val5	7.62	3.82	2.30	γ-CH_3 0.96, 1.05	65.1
Leu6	8.39	4.10	1.83	γ-CH 1.61 δ-CH_3 0.89, 0.93	57.0
Gly7	8.44	3.90			45.8
Ser8	7.77	4.39	4.09, 4.23		60.9
Val9	8.36	3.75	2.33	γ-CH_3 0.97, 1.08	66.1
Ala10	8.68	4.06	1.57		54.9
Lys11	7.86	4.03	1.82, 1.91	γ-CH_2 1.45 δ-CH_2 1.68 ε-CH_2 2.95	57.9
His12	7.93	4.61	3.42	H2 8.61 H4 7.46	57.1
Val13	8.34	4.10	2.14	γ-CH_3 0.99, 1.08	64.5
Leu14	8.54	4.35	1.99	γ-CH 1.55 δ-CH_3 0.89, 0.94	58.5
Pro15	–	4.28	1.42, 2.28	γ-CH_2 1.90, 2.05 δ-CH_2 3.34, 3.74	62.7
His16	7.90	4.59	3.40	H2 8.62 H4 7.59	55.6
Val17	7.95	4.29	2.16	γ-CH_3 1.00, 1.05	64.8
Val18	8.20	3.90	2.17	γ-CH_3 0.97, 1.10	66.9
Pro19	–	4.28	1.81, 2.35	γ-CH_2 1.94, 2.16 δ-CH_2 3.48, 3.67	64.8
Val20	7.07	3.81	2.38	γ-CH_3 1.02, 1.12	65.1
Ile21	7.91	3.76	2.05	γ-CH_2 1.15, 1.68 γ-CH_3 0.94 δ-CH_3 0.83	64.2
Ala22	8.72	4.02	1.46		54.3
Glu23	8.00	4.12	2.13, 2.20	γ-CH_2 2.52	56.8
His24	7.95	4.49	3.28, 3.44	H2 8.49 H4 7.44	56.8
Leu25	8.06	4.31	1.83	γ-CH 1.61 δ-CH_3 0.88, 0.88 $CONH_2$ 6.82, 7.23	54.7

RESULTS

Antimicrobial effects of caerin 1.1 and its variants. The ability of caerin 1.1 and some of its synthetic variants, along with caerin 1.3, to prevent the growth of a variety of micro-organisms was tested and the results are summarised in Table 1. Caerin 1.3 is a naturally ocurring variant of caerin 1.1 with Lys11 substituted by a Gln (Stone et al., 1993). The data are represented as MIC values with a lower value indicative of greater activity. As is apparent from these data, the all-D-amino acid form of caerin 1.1 has almost identical activity to the natural form of the peptide. On the other hand, substitution of either or both of the Pro residues with Gly leads to peptides with overall reduced activity. Interestingly, the single amino acid substitution in caerin 1.3 gives a peptide that has high specificity for *M. luteus* bacteria.

CD spectroscopy. CD spectra were acquired on caerin 1.1 in increasing concentrations from 0 to 50% (by vol.) trifluoroethanol in H_2O. As can be seen from Fig. 1, at concentrations up to 20% trifluoroethanol, caerin 1.1 exhibited a CD spectrum characteristic of a peptide that has little overall preferred conformation (or random coil structure), i.e. a broad minimum around 200 nm is observed. In increasing the trifluoroethanol concentration to 30% (by vol.), however, the CD spectrum underwent a marked change to one indicative of a predominance of α-helix (i.e. two minima in the vicinity of 208 and 222 nm). At 40% and 50% trifluoroethanol, the CD spectra were very similar with a greater ellipticity being observed at these minima compared to the spectrum at 30% trifluoroethanol. Peptides with a pronounced helical propensity will adopt maximal helical conformation at relatively low (30–50% by vol.) trifluoroethanol concentration (Sönnichsen et al., 1992). It should be noted that 30% and 50% (by vol.) trifluoroethanol/H_2O correspond to a mole fractions of 10:90 and 20:80 respectively, i.e. to relatively small amounts of trifluoroethanol on a molar basis. It would seem from the CD results, therefore, that caerin 1.1 has a high tendency to adopt a mainly helical conformation.

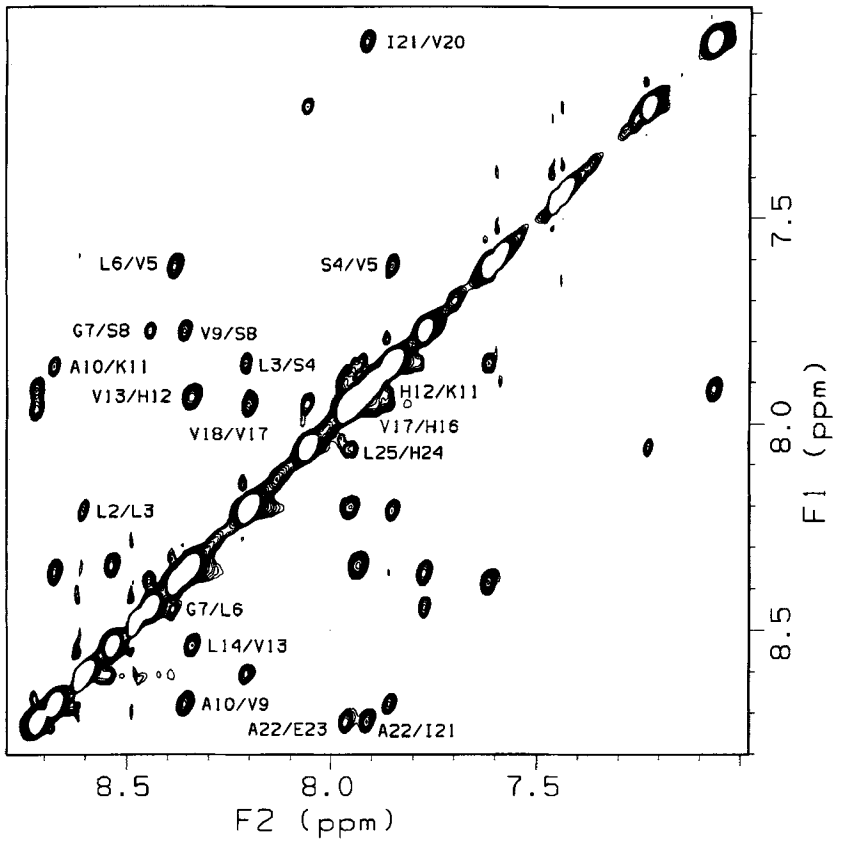

Fig. 2. NH to NH region of a NOESY spectrum (mixing time = 150 ms) of caerin 1.1 in 50% (by vol.) trifluoroethanol. NOEs between sequential NH protons are indicated.

NMR spectroscopy and structure generation. On the basis of the CD results, NMR spectra were acquired on caerin 1.1 under conditions in which maximal secondary structure was present, i.e. 50% (by vol.) trifluoroethanol. The ^{1}H-NMR spectrum was assigned via standard methods using the sequential assignment procedure of Wüthrich (1986) which involved the combined use of DQF-COSY, TOCSY and NOESY spectra. The protonated ^{13}C-NMR resonances were assigned via an HSQC spectrum from the one-bond correlations of the ^{13}C resonances to the assigned ^{1}H resonances. The assignments for all the ^{1}H resonances and the α-CH ^{13}C resonances are given in Table 2.

Fig. 2 shows the NH region of a NOESY spectrum in which a series of sequential NH to NH NOEs [$d_{NN}(i,i+1)$] were observed along the length of the polypeptide with gaps at the expected positions of the two proline residues (Pro15 and Pro19). The presence of strong $d_{NN}(i,i+1)$ NOEs is consistent with a helical structure for the peptide (Wüthrich, 1986). The various types of NOEs observed for caerin 1.1 are summarised in Fig. 3. It is apparent from this figure that the strong $d_{NN}(i,i+1)$ NOEs were complemented by weaker sequential NOEs between NH protons and preceding α-CH protons [$d_{\alpha N}(i,i+1)$]. In addition, a series of NOEs from residues three and four amino acids distant in the peptide [$d_{\alpha N}(i,i+3)$, $d_{\alpha\beta}(i,i+3)$ and $d_{\alpha N}(i,i+4)$] were present, although there were some interruption of this pattern in the vicinity of Lys11 (Fig. 3). Finally, five $d_{NN}(i,i+2)$ NOEs were also observed (at a lower contour level to that shown in Fig. 2). When taken together, the above NOEs and their intensities are consistent with helical secondary structure being present along the majority of the polypeptide chain (Wüthrich, 1986). Similarly, the NH protons whose $^3J_{NH\alpha}$ values could be measured from 1D ^{1}H-NMR spectra acquired at various temperatures, mostly had values ($\leq$5 Hz) that were consistent with helical structure (Fig. 3).

Other evidence for helical structure in caerin 1.1 came from an examination of cross-peaks associated with the six Val residues. In a helical region, the prochiral γ-CH$_3$ protons of a Val residue can be stereospecifically assigned (Zuiderweg et al., 1985). Thus, providing that the α-CH to β-CH coupling constant is larger than about 12 Hz, the methyl group with the more intense NOESY cross peak to the NH has *S* prochirality. Except for Val13, where the DQF-COSY α-CH to β-CH cross-peak overlapped that for Glu23, it was possible to assign stereospecifically the five other Val γ-CH$_3$ resonances. In all cases, the more intense of the two NH to γ-CH$_3$ NOESY cross-peaks was at lower field which was therefore assigned as the *S* prochiral γ-CH$_3$.

The predominance of helical structure in caerin 1.1 was also indicated from an examination of the deviation from random coil chemical shift values (Wüthrich, 1986; Wishart et al., 1995) of the ^{1}H and ^{13}C α-CH resonances. Although a complete set of random coil chemical shifts are not available for amino acids in trifluoroethanol, those which have been tabulated (Merutka et al., 1995) indicate that there is little difference between random coil chemical shifts in trifluoroethanol and water. Accordingly for caerin 1.1 in trifluoroethanol, a comparison was made with random coil chemical shifts determined in water (Wishart et al., 1995). For a window of $n = \pm 2$ residues (Pastore and Saudek, 1990), the smoothed plots for the ^{1}H resonances showed a distinct upfield shift and those for the ^{13}C resonances a distinct downfield shift along the majority of the peptide with the exceptions being in the vicinity of Pro15 and at the N- and C-termini (Fig. 4). The directions of these deviations from random coil

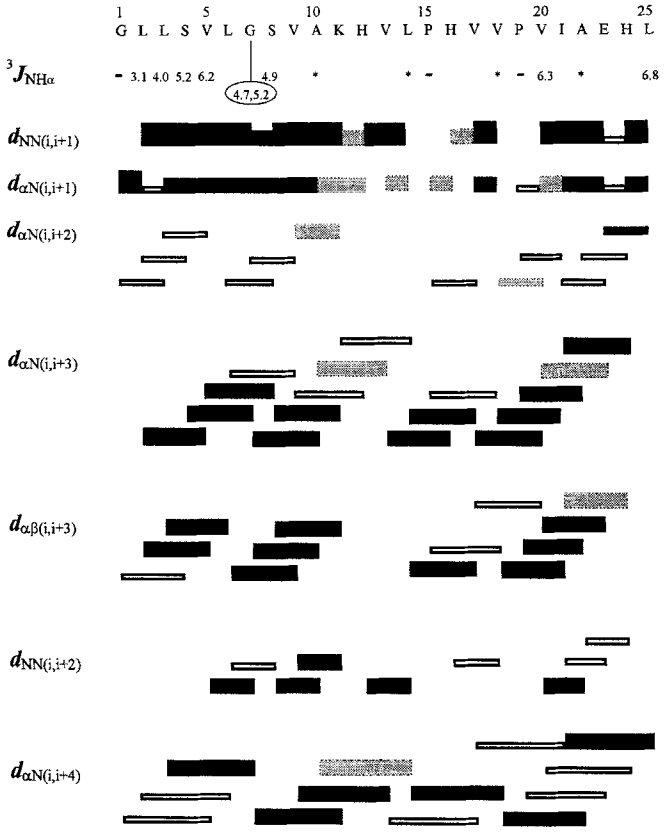

Fig. 3. A summary of NOEs used for structure calculation of caerin 1.1 in 50% (by vol.) trifluoroethanol. The thickness of bars indicates the relative strength of NOEs (strong, medium or weak). Clearly defined NOE cross-peaks that overlapped by more than 15% with other cross-peaks, and were therefore not used in the structure calculations, are indicated by a greyscale connectivity. Unfilled boxes represent connectivities that could not be unequivocally assigned due to overlap, e.g. with an intra-residue NOE. The $^3J_{NH\alpha}$ values, where possible as determined from 1D NMR spectra acquired at various temperatures, are indicated. Those with an asterisk indicate broad NH resonances whose $^3J_{NH\alpha}$ values could not be determined accurately.

chemical shift ^1H and ^{13}C α-CH values are consistent with helical structure in the vicinity of Leu6 and Ile21 (Wishart et al., 1991). The greater random-coil nature of the α-CH chemical shifts in between these regions (i.e. near Pro15) suggests that the middle portion of the molecule does not have as strong helical preference, and that this region is more flexible (Wishart et al., 1991).

Indeed, the conclusions derived from an examination of the NMR data presented in Figs 2–4 were confirmed when the NOE data were used as input for the calculation of the solution structure of caerin 1.1. Twenty structures were generated by distance geometry followed by RMD. The first ten of these structures were then arbitrarily selected for close examination and some statistics on these structures are presented in Table 3. During the course of a structure generation the error function was typically 4000 ± 700 after embedding, dropping to around the final error level after RMD (Table 3). Where energy minimisation was performed after RMD (when the error function was less than the failure level), the error function was generally lowered by only a small amount except for structure 4 where a slight increase occurred.

Eight structures had error functions close to or less than the chosen failure level, but two (structures 2 and 7) displayed poorer convergence with error function values approximately twice the failure level. Close examination of the restraint violations for all ten structures revealed, first, that the original chirality restraints were always retained, except for the (expected) departures from ideal planarity. Second, chirality and van der Waals violations always made significantly less contribution (about an order of magnitude) to the error function whereas distance restraint violations were the major contributor. Distance violations were almost always intra-residue upper-bound violations (except for structures 2 and 7) and, for the ten arbitrarily chosen structures, the maximum violation ranged over 38–57 pm and was invariably associated with Pro15, most commonly involving one of the β-CH_2 to δ-CH_2 upper-bound restraints. Similar behaviour had been noted during preliminary structure generation and close attention was therefore paid to the veracity of the Pro assignments as well as careful delineation of the footprint of the contours in the NOESY spectrum which has a resultant effect on volume integrations. In addition, selective loosening of the NOE distance restraints for the Pro residues was attempted. After performing these corrections, however, the NOE distance restraints were consistently violated in the vicinity of Pro15.

Third, for structures 2 and 7, the poor convergence during RMD was due to violations of small lower-bound restaints (that were not Van der Waal's terms). Last, during structure generation, close attention was also paid to those residues showing the maximum displacement at selected time steps (every 100 steps) of the RMD. If these displacements were completely at random then each residue in caerin 1.1 would be expected to display maximum displacements for 4% of the total time steps, on average. Attention was focused on Pro15 and Pro19 and the two residues (Lys11, His16), close to the region of wider variation in the (ϕ, ψ) torsion angles for the ten structures (see below). On average, only His16 displayed a pronounced higher frequency of maximum displacements (about 7%).

Fig. 5 shows one of these structures (number 6) obtained after the structure-generation protocol. It, along with all the other structures, exhibited a predominantly helical array along the entire molecule. In the structure shown in Fig. 5 there is, however, a distinct bend in the vicinity of His12. Indeed, when the ten structures of caerin 1.1 were compared, marked conformation variability was observed in this region (His12–His16) so that two distinct regions of helicity (Leu2–Lys11 and Val17–His24) were present interdispersed with a region of greater conformational flexibility that in all structures had a distorted but non-superimposable helical appearance. Fig. 6 demonstrates this well where the ten structures are aligned from Leu2 to Lys11 on the bottom overlay and from Val17 to His24 on the top overlay. As is apparent from Fig. 6, both of these regions have highly helical character which is quantifyable in that both helices had small average pairwise root-mean-square deviation (RSMD) values of 0.0075 ± 0.0023 nm^2 and 0.0048 ± 0.0014 nm^2 respectively over the ten structures. Plots of backbone torsion angles (ϕ, ψ) versus amino acid sequence (Fig. 7) also reveal conformational variability in the central portion (and at the peptide extremities). Thus in the helical regions, (ϕ, ψ) values are, in the main, in the expected regime of $(-60°, -60°)$ for an α-helix whilst outside these regions large deviations from these (ϕ, ψ) values are found.

The presence of helices in these two regions is also consistent with the observation of Wishart et al. (1991) that the helix dipole influences the NH chemical shifts of residues at the N- and C-terminal of the helix such that the former have a markedly lower chemical shift than the latter. Thus, for the N-terminal helix in caerin 1.1, the average NH chemical shift for Gly1 to Leu3 (i.e. the $N-1$ to $N+1$ residues) was 8.41 ppm and for Ala10 to His12 (i.e. the C−1 to C+1 residues), it was 8.16 ppm.

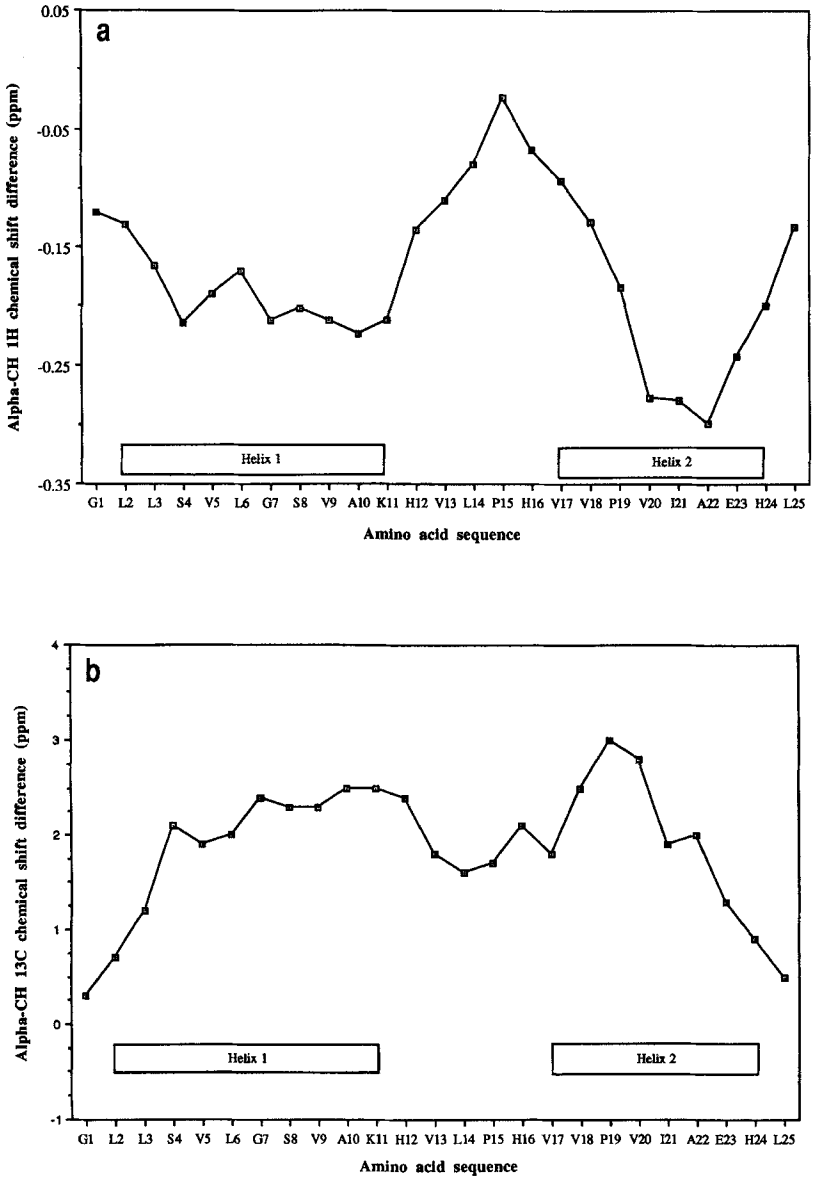

Fig. 4. Deviation from random coil chemical shifts (Wishart et al., 1995) for the (a) ^{1}H and (b) ^{13}C α-CH resonances of caerin 1.1 in 50% (by vol.) trifluoroethanol. A negative deviation indicates an upfield chemical shift compared to the random coil value. The chemical shifts were smoothed over a window of $n = \pm 2$ residues (Pastore and Saudek, 1990). No corrections were made for the effect on the α-CH chemical shifts of Leu14 and Val18 due to their subsequent Pro residues, as these effects have only been quantified for random coil peptides in aqueous solvent (Wishart et al., 1995).

Table 3. Structure parameters following distance geometry and RMD calculations on caerin 1.1. The parameter ⟨no. violations⟩ is the number of distance or contact violations that exceeded 1% of the total distance or contact contribution to the final error function.

Parameter	Value
No. of structures	10
Error function range	1.51 − 4.74
⟨Error function⟩	2.36 ± 1.11
Distances:	
⟨No. violations⟩	18.9 ± 3.3
⟨Max. violations⟩	49 ± 6 pm
Van der Waals contacts:	
⟨No. violations⟩	21.7 ± 2.2
⟨Max. violations⟩	33 ± 7 pm

Likewise for the C-terminal helix, these values were 8.12 and 7.99 ppm for His16 to Val17 and Glu23 to Leu25 respectively.

Finally, NH temperature coefficients were measured for caerin 1.1 in the range from 25° − 54 °C in an endeavour to glean information on the involvement or otherwise of NH protons in intra-molecular hydrogen bonding. 1D ^{1}H-NMR spectra were acquired over this temperature range with TOCSY spectra being recorded at 10 °C increments to facilitate assignment. In water, a high temperature coefficient (> 5 ppb/°C) is usually ascribed to a peptide NH proton that is not involved in intra-molecular hydrogen bonding interactions, i.e. one that is participating in hydrogen bonds to the solvent water molecules. On the other hand, a low temperature coeficient (< 5 ppb/°C) implies an intra-molecular hydrogen bond is present. The temperature coefficients for caerin 1.1 in 50% trifluoroethanol are presented in Fig. 8. As can be seen, these data show no consistent variation as would be expected if the above rationale were expected to

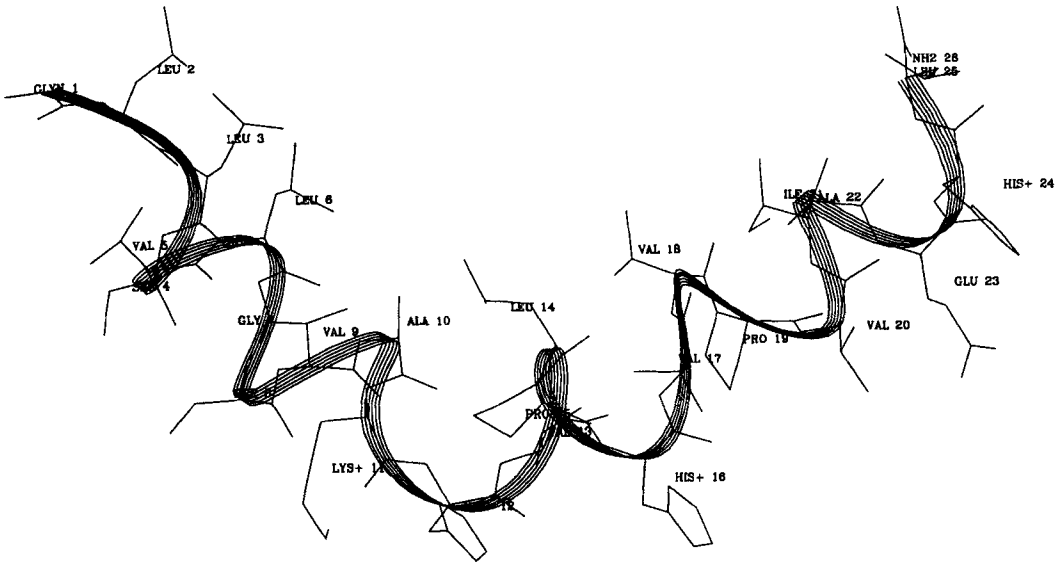

Fig. 5. Conformation number 6 of caerin 1.1 obtained after distance geometry and RMD calculations. A ribbon is drawn along the polypeptide backbone. The two helical regions are apparent from this representation along with the distinct spatial distribution of hydrophobic and hydrophilic amino acids on the concave and convex sides of the peptide, respectively.

hold, e.g. the helical regions of the peptide in which the NH protons, after the first four residues, are involved in hydrogen bonds, have widely different NH temperature coefficients. Similarly inconsistent behaviour has been found for the temperature coefficients of the helical ribonuclease S peptide in 50% trifluoroethanol (Storrs et al., 1992). The opposite pattern, however, to that described above for NH protons in water can be observed for the temperature coefficients of helical peptides in 100% trifluoroethanol solutions (Carver et al., 1997). It may be, therefore, that in aqueous/trifluoroethanol mixtures NH temperature dependence arises from a combination of factors (i.e. exposure to solvent and involvement in hydrogen bonds) which makes interpretation of their coefficients difficult.

DISCUSSION

By placing the amino acid sequence of caerin 1.1 on an Edmundsen helical wheel projection, it is apparent that the peptide can adopt an amphipathic α-helix from Gly1 to Pro15 (Stone et al., 1992b), and from His16 to Leu25, with the centre of the latter helix being shifted in orientation by approximately 140° compared to the former. Many studies have shown that an amphipathic helix is a common structural motif for interaction of peptides with membranes. The results presented in this paper show that in trifluoroethanol, caerin 1.1 forms two well-constructed amphipathic helices (Leu2–Lys11 and Val17–His24) which are separated by a short, central region of a helical nature and greater flexibility. Trifluoroethanol is a solvent which preferably adopts hydrogen bonds within itself (Kreuger and Mettee, 1964) and thereby promotes intra-molecular hydrogen bonds within its solutes. In the latter sense, it is thus a membrane-mimicking solvent. Previous studies have shown that trifluoroethanol only induces structure in polypeptide regions that have a propensity to adopt secondary structure (Sönnichsen et al., 1992). The amphipathic helical conformation of caerin 1.1 determined herein, therefore, may be the one that the peptide adopts when interacting with membranes. Indeed for magainin, solid-state NMR studies of the peptide incorporated into lipid bilayers show that it adopts a helical conformation aligned parallel to the plane of the membrane (Bechinger et al., 1991, 1993; Ramamoorthy et al., 1995). Fig. 5 demonstrates that the two helical regions are oriented such that their sidechains form a continuous hydrophobic face on the concave side of the peptide and a hydrophilic side on the convex side, i.e. the peptide has distinct polar and non-polar faces. All ten structures also had an overall amphipathic charge distribution which was achieved in a varied manner via alteration in flexibility of the central region. In summary, therefore, the observed flexibility in the central region of caerin 1.1 (His12–His16) enables the molecule to undergo the reorientation required for the distribution of amino acids to ensure two distinct (polar and non-polar) faces for the molecule.

It is of interest to examine the effects of specific amino acids on the structure of caerin 1.1. Firstly, Gly7 is in the middle of the N-terminal stretch of α-helix. Glycine is a well-known helix breaker and there is a distinct structural preference for Gly at the end of a helix (Richardson and Richardson, 1988). For caerin 1.1, this is not the case as the helix is contiguous from Leu2 to Lys11. On the other hand, it is apparent from the greater spread of the ϕ and ψ angles in the vicinity of Gly7 compared to nearby residues in the ten structures (Fig. 7) that there is some small disruption to the helix in this region. The α-CH ^{1}H chemical shifts of Gly7 and Ser8 reflect this deviation in that they are shifted upfield by less than 0.1 ppm compared to random coil values, whereas their flanking residues have upfield shifts indicative of helicity of greater than 0.25 ppm. Furthermore, this structural variation is in the vicinity of Gly7 is apparent from the larger RMSD values of the N-terminal helix compared to the C-terminal helix and the greater scatter of the N-terminal helix in the structures shown in Fig. 6.

Secondly, positively charged amino acids are often found at the C-terminal of helices (Richardson and Richardson, 1988) and the presence of Lys11, His12 and His24 at the ends of both helical sections is consistent with this observation. Their positive charge helps to stabilise the helix dipole which, of course, is of opposite charge at the C-terminal of the helix. Furthermore, when Lys is a C-terminal residue, it can utilise its sidechain amino group to form a hydrogen bond to the backbone carbonyl of the amino acid four residues before it in the sequence (Esposito et al., 1997). Understandably, this interaction leads to an enhancement of stability for the helix. For caerin 1.1, the positive charge on the sidechain of Lys11 may also be involved in

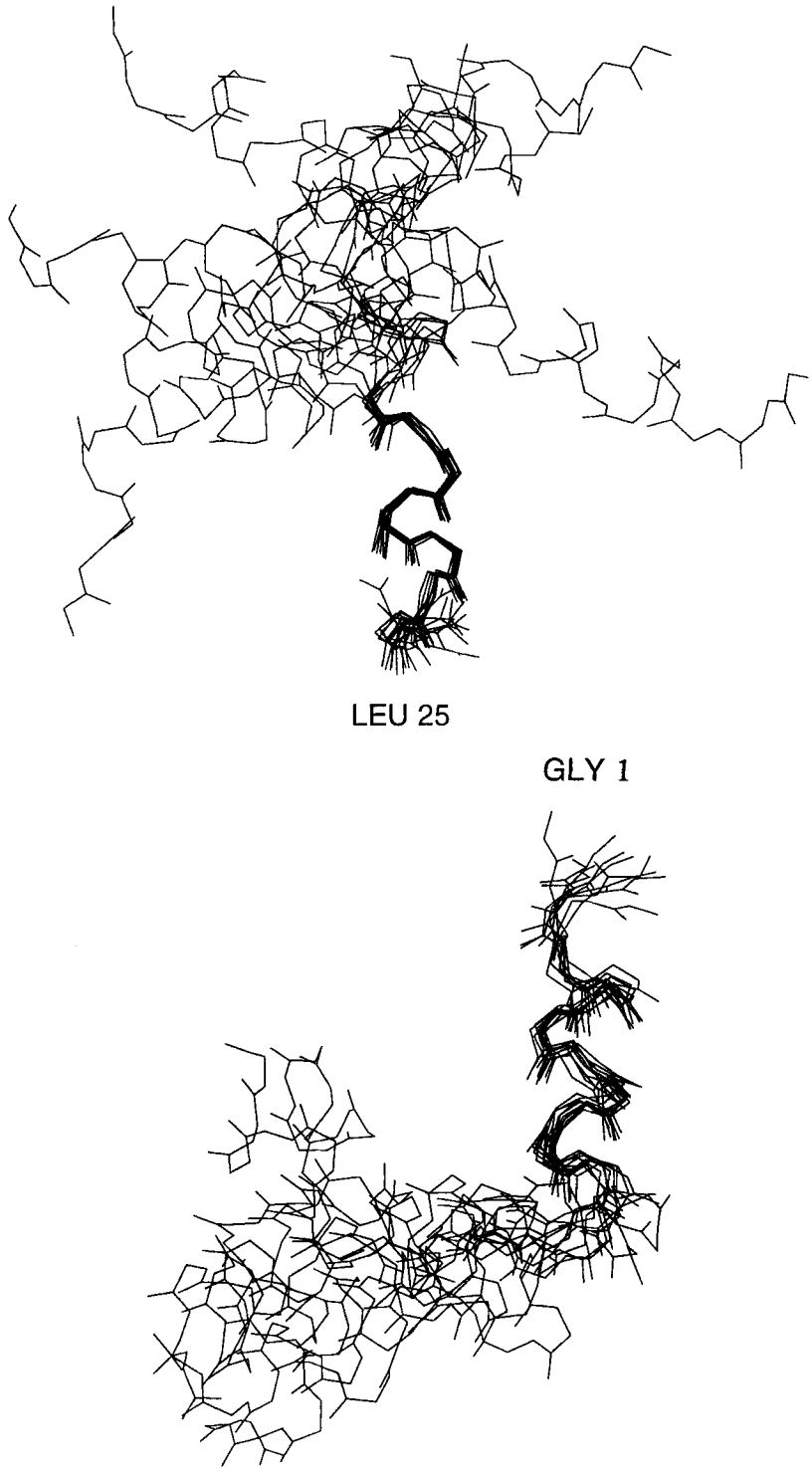

Fig. 6. Ten structures of caerin 1.1 obtained after distance geometry and RMD calculations. The bottom overlay shows the ten structures aligned from Leu2 to Lys11 and the top overlay shows the structures aligned from residues Val17 to His24.

the interaction of the peptide with anionic phospholipids. In general, it is believed that positively charged amino acids play an important role in the mechanism of action of antimicrobial peptides via their ability to interact with the anionic phospholipids which are selectively present in high concentrations in bacterial membranes (Jacob and Zasloff, 1994). In the case of caerin 1.1, Lys11 being at the end of the helix and at the start of the flexible central region, may facilitate this interaction. The importance of its positive charge is apparent from the biological results where the substitution of Lys11 with Gln (to give uncharged caerin 1.3) leads to a marked reduction in activity for most organisms tested (Table 1). In the same vein, the three His may have a similar electrostatic role in interacting with anionic phospholipids although, at physiological pH, their imidazole sidechains are most likely to be mainly deprotonated and uncharged and hence this effect is probably not as significant as

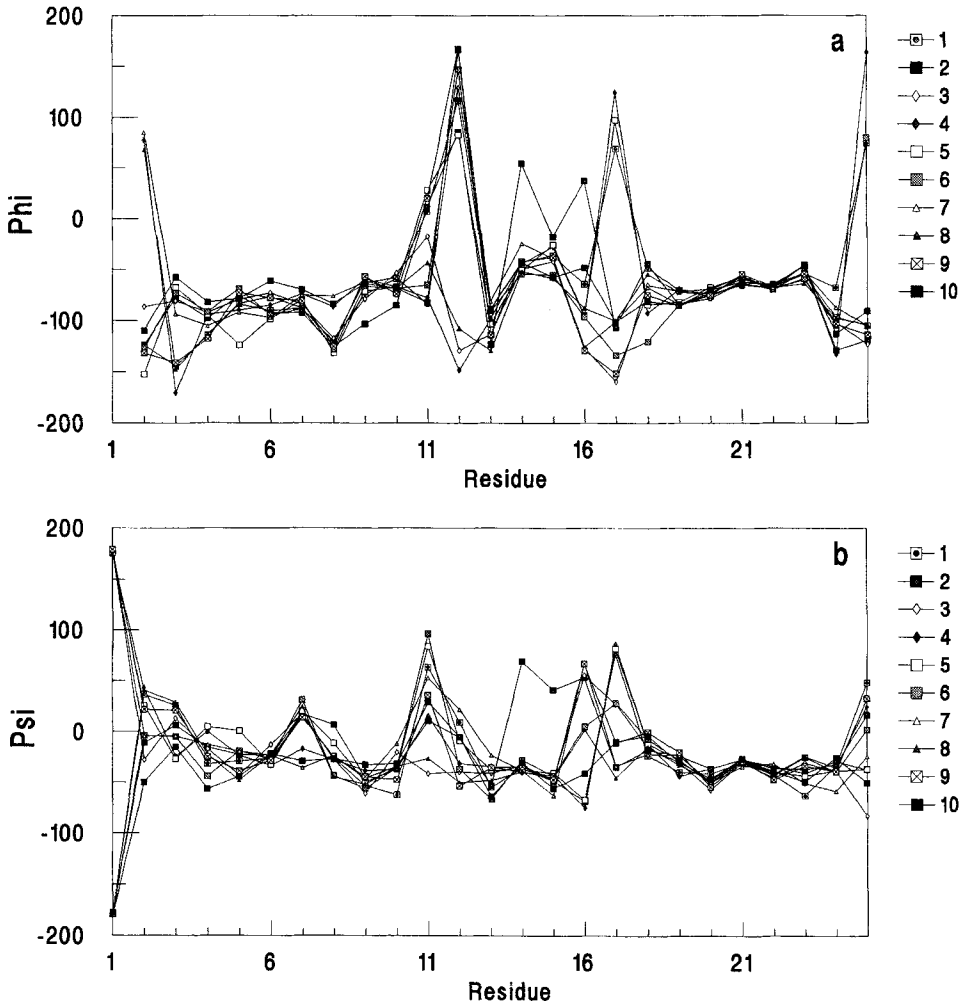

Fig. 7. Plots of (a) ϕ and (b) ψ backbone torsion angle distribution versus amino acid sequence for caerin 1.1 as obtained for each of the ten structures shown in Fig. 6.

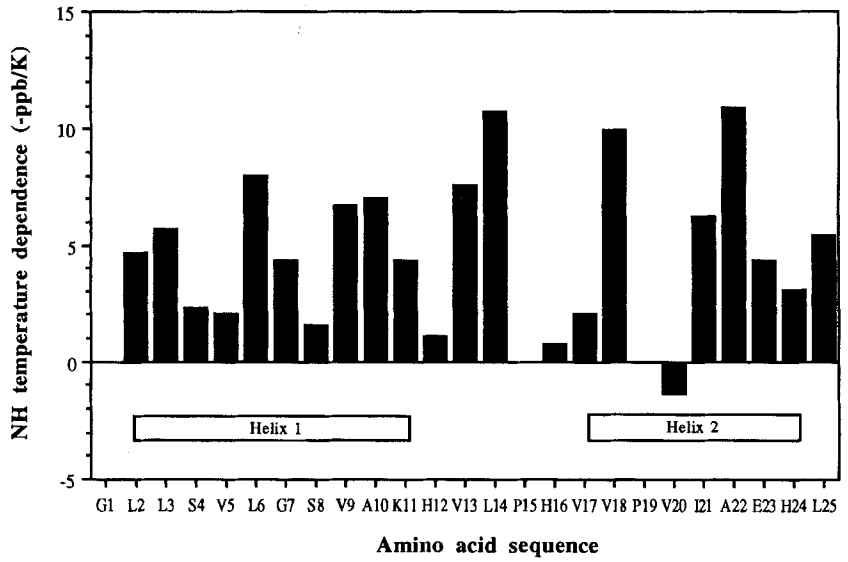

Fig. 8. Plot of temperature coefficients of the NH resonances versus the amino acid sequence of caerin 1.1 in 50% (by vol.) trifluoroethanol.

that for Lys11. The selectivity of caerin 1.3 for *M. luteus* (Table 1) may arise from the unique composition of the cell wall of this bacterium. Thus, in contrast to *S. aureus* which is of the same family, *M. luteus* does not contain negatively charged and phosphate-containing teichoic acids in its outer cell wall (Kocur, 1986). Furthermore, as for other gram-positive bacteria, peptidoglycan units make up the majority of the cell wall constituents of these two bacteria and, amongst these units, *M. luteus* contains positively charged Lys_5 linkers in contrast to *S. aureus* which has a Gly_5 linker (Baird-Parker, 1974). The cell wall of *M. luteus* is therefore mainly positively charged whereas that of *S. aureus* contains many negative charges. Thus, charge variation of cell walls in bacteria may be a significant factor in determining their interaction with positively charged caerin 1.1 and neutral caerin 1.3.

Thirdly, caerin 1.1 has two Pro residues, at positions 15 and 19. Proline, due to the absence of an NH proton, a cannot form hydrogen bond and is therefore statistically rarely found in the middle of helices but is reasonably common in the first four amino acids of a helix (Richardson and Richardson, 1988). When Proline is present in the middle of helices it provides a kink to the helix (Woolfson and Williams, 1990) as is observed in the membrane-interacting peptides, alamethicin (Esposito et al., 1987) and melittin (Bazzo et al., 1988). For caerin 1.1, the presence of Pro15 in the flexible central region would facilitate the conformational rearrangement required to ensure the similar positioning of polarity of the two helices. Flexibility in this region is also indicated by the predominance of violations in the structure calculations which involved Pro15. Thus, the variation in correlation time of this central region relative to the rest of the molecule would cause errors in measurement of NOE intensities which would be reflected in violations involving Pro15.

Pro19 is at the start of the second helix so its lack of an NH proton would not upset the hydrogen bonding pattern of the helix and thereby its ordered progression (Richardson and Richardson, 1988; Presta and Rose, 1988). Indeed, the structures shown in Figs 5 and 6 and the backbone torsional angle distribution (Fig. 7) show that the C-terminal helix is quite uniform. Activity data (Table 1) demonstrate that alteration of these Pro residues to Gly has a large effect on the activity of the peptide. Thus, when either of these Pro is replaced with a Gly, the activity is severely reduced and the activity of the variant is similar to that of the peptide in which both Pro are substituted by Gly. For the peptide in which the first Pro is altered, the added flexibility introduced with the Gly residue could distrupt the optimal amphipathic orientation of the two helices whilst the presence of a Gly at the start of the C-terminal helix would be very disruptive to the order of the second helix. Interestingly, in all caerin 1 peptides sequenced to date, Pro15 and Pro19 are conserved (Steinborner et al., 1996; Stone et al., 1992a,b, 1993; Waugh et al., 1993), implying that both Pro residues are important for functionality of caerin 1.1.

The solution-state NMR structures in hydrophobic solutions of some other antimicrobial peptides have also shown that they adopt a dual amphipathic helical arrangement with central flexibility. Thus, the related peptides, cecropin A (Holak et al., 1988) and sarcotoxin IA (Iwai et al., 1993) have long N- and C-terminal helices (of 16 and 13 amino acids respectively in cecropin A) which are separated by a flexible hinge region. As for caerin 1.1, the flexible region in cecropin A is characterised by having a Pro residue whilst sarcotoxin IA has two Gly residues in this region. As expected for cecropin A and sarcotoxin IA, an almost-complete series of (i,i+3) and (i,i+4) NOEs are observed along the peptide in the two helical regions (Holak et al., 1988; Iwai et al., 1993). In the spanning regions between the helices, however, there are only a few such NOEs which suggests that these regions have a much poorer helical tendency and greater flexibility. Along the polypeptide chain of caerin 1.1 a very similar pattern of NOEs is observed to those for cecropin A and sarcotoxin IA (Fig. 3). In particular, there is a noticeable interruption in the pattern of structure-defining (i,i+2), (i,i+3) and (i,i+4) NOEs in the central region. As expected, therefore, all three peptides have an analogous overall structural arrangement. The antibiotic peptide, buforin II, also has two helical regions although the N-terminal one is short (four amino acids) and distorted due to it ending in a Pro residue prior to the peptide entering into a well-defined C-terminal helix (Yi et al., 1996). As discussed above, in the membrane channel-forming peptides, melittin (Bazzo et al., 1988) and alamethicin (Esposito et al., 1987), the central Pro residues have a less disruptive effect to the helix but they still cause a marked kink in the overall helical pattern and a concomitant increase in flexibility. Thus, the presence of central flexibility in all these peptides may be a common feature of many antimicrobial peptides to allow for optimal orientation of the amphipathic helices with respect to the membrane surface. This arrangement is not unique to antimicrobial peptides since a similar structural arrangement is observed in the non-antimicrobial armadillo peptide from the APC protein where the central flexible region between the two helices has a significant number of (i,i+3) and (i,i+4) NOEs (Hirschl et al., 1996).

Physico-chemical studies of other antibiotic peptides have provided convincing evidence that their mechanism of action involves disruption of bacterial membranes via a carpet-like mechanism (reviewed by Shai, 1995). In this mechanism, the peptides bind in an α-helical form with their axes parallel to the membrane and, above a critical concentration, form a carpet-like monolayer on the membrane surface. Transient holes are subsequently formed in the membrane leading to cell lysis. There is no evidence that antimicrobial peptides form *trans*-membrane channels via a barrel-stave mechanism (Shai, 1995) as is the case for some ionophoric or cytolytic peptides (e.g. alamethicin and melittin). The structural conclusions for caerin 1.1 from this work are similar to those for other antimicrobial peptides, i.e. the peptide forms an amphipathic helix in a hydrophobic environment. Furthermore, the net positive charge of caerin 1.1 seems to be important to its function since all caerin 1.1 variants (apart from the uncharged caerin 1.3) are positively charged at neutral pH. As discussed above, the absence of the positive charge in caerin 1.3 leads to a peptide with much less broad-spectrum antimicrobial activity (Table 1).

Like the all-L-amino acid native caerin 1.1, its all-D-amino acid variant can also potentially form an amphipathic helix (but of opposite, left-handed sense). The activities of these two caerin 1.1 peptides are very similar (Table 1) which is strong circumstantial evidence that the action of caerin 1.1 involves interaction with the bacterial membrane via an amphipathic helix (i.e. there is no interaction of the peptide with chiral sites, e.g. receptors or enzymes). Likewise, the L- and D-amino acid derivatives of other antimicrobial peptides have very similar activities (Barra and Simmaco, 1995). It would seem, therefore, that caerin 1.1, like all other antibiotic peptides studied to date, interacts with membranes via the carpet-like mechanism. In the future, the design of more potent caerin 1.1 analogues should take into account the necessity for any changes to be compatible with the carpet-like mechanism and that these alterations be undertaken so as not to alter, but to enhance, the overall structural features of caerin 1.1.

This work was supported, in part, by a grant from the Australian Research Council (to JHB). We thank Drs Robyn Lindner and Graham Ball for assistance with acquisition of the NMR spectra. Dr Lindner is

also thanked for preparing Fig. 1. Industrial Research Ltd, New Zealand, provided leave of absence for HW which enabled this work to be carried out in Wollongong.

REFERENCES

Baird-Parker, A. C. (1974) in *Bergey's manual of determinative bacteriology*, 8th edn, (Buchanan, R. E. & Gibbons, N. E., eds) pp. 480–490, Williams and Wilkins, Baltimore MD.

Barra, D. & Simmaco, M. (1995) Amphibian skin: a promising resource for antimicrobial peptides, *Trends Biotech. 13*, 205–209.

Bazzo, R., Tappin, M. J., Pastore, A., Harvey, T. S., Carver, J. A. & Campbell, I. D. (1988) The structure of melittin. A ^{1}H-NMR study in methanol, *Eur. J. Biochem. 173*, 139–146.

Bechinger, B., Kim, Y., Chirlian, L. E., Gesell, J., Neumann, J.-M., Montal, M., Tomich, J., Zasloff, M. & Opella, S. J. (1991) Orientations of amphipathic helical peptides in membrane bilayers determined by solid-state NMR spectroscopy, *J. Biomol. NMR 1*, 167–173.

Bechinger, B., Zasloff, M. & Opella, S. J. (1993) Structure and orientation of the antibiotic peptide magainin in membranes by solid-state nuclear magnetic resonance spectroscopy, *Protein Sci. 2*, 2077–2084.

Bevins, C. L. & Zasloff, M. (1990) Peptides from frog skin, *Annu. Rev. Biochem. 59*, 395–414.

Carver, J. A., Esposito, G., Viglino, P., Fogolari, F., Guichard, G., Briand, J.-P., Van Regenmortel, M. H. V., Brown, F. & Mascagni, P. (1997) Structural basis between retro-inverso and parent peptides. Molecular basis for the biological activity of a retro-inverso analogue of the immunodominant fragment of VP1 coat protein from foot-and-mouth disease virus, *Biopolymers 41*, 569–590.

Davis, D. G. & Bax, A. (1985) Assignment of complex ^{1}H NMR spectra via two-dimensional homonuclear Hartmann-Hahn spectroscopy, *J. Am. Chem. Soc. 107*, 2820–2821.

Erspamer, V. (1994) Bioactive secretions of the amphibian integument, in *Amphibian biology. The integument*, vol. 1, pp. 178–350, Surrey Beatty, Chipping Norton, Australia.

Esposito, G., Carver, J. A., Boyd, J. & Campbell, I. D. (1987) High-resolution ^{1}H NMR study of the solution structure of alamethicin, *Biochemistry 26*, 1043–1050.

Esposito, G., Dhanapal, B., Dumy, P., Varma, V., Mutter, M. & Bodenhausen, G. (1997) Lysine as a helix C-capping residue in a synthetic polypeptide, *Biopolymers 41*, 27–35.

Griesinger, C., Otting, G., Wüthrich, K. & Ernst, R. R. (1988) Clean TOCSY for ^{1}H spin system identification in macromolecules, *J. Am. Chem. Soc. 110*, 7870–7872.

Havel, T. F. (1991) An evaluation of computational strategies for use in the determination of protein structure from distance constraints obtained by nuclear magnetic resonance, *Prog. Biophys. Mol. Biol. 56*, 43–78.

Hirschl, D., Bayer, P. & Müller, O. (1996) Secondary structure of an armadillo single repeat from the APC protein, *FEBS Lett. 383*, 31–36.

Holak, T. A., Engström, Å., Kraulis, P. J., Lindeberg, G., Bennich, H., Jones, T. A., Gronenborn, A. M. & Clore, G. M. (1988) The solution conformation of the antibacterial peptide cecropin A: a nuclear magnetic resonance and dynamical simulated annealing study, *Biochemistry 27*, 7620–7629.

Iwai, H., Nakajima, Y., Natori, S., Arata, Y. & Shimada, I. (1993) Solution conformation of an antibacterial peptide, sarcotoxin IA, as determined by ^{1}H-NMR, *Eur. J. Biochem. 217*, 639–644.

Jacob, L. & Zasloff, M. (1994) Potential therapeutic applications of magainins and other antimicrobial agents of animal origin, *Ciba Found. Symp. 186*, 197–223.

Jeener, J., Meier, B. H., Bachman, P. & Ernst, R. R. (1979) Investigation of exchange processes by two-dimensional NMR spectroscopy, *J. Chem. Phys. 71*, 4546–4553.

John, B. K., Plant, D., Webb, P. & Hurd, R. E. (1992) Effective combination of gradients and crafted RF pulses for water suppression in biological samples, *J. Magn. Reson. 98*, 200–206.

Jorgensen, J. H., Cleeland, R., Craig, W. A., Doern, G., Ferraro, M. J., Fingold, S. M., Hansen, S. L., Jenkins, S. G., Novick, W. J., Pfaller, M. A., Preston, D. A., Reller, L. B. & Swenson, J. M. (1993) Methods for dilution antimicrobial susceptibility tests for bacteria that grow aerobically - third edition; approved standard, *National Committee for Clinical Laboratory Standards 13*, 1–12. Document M7-A3, ISBN 1-56238-209-8. ISSN 0273-3099.

Kay, L. E., Keifer, P. & Saarinen, T. (1992) Pure absorption gradient enhanced heteronuclear single quantum correlation spectroscopy with improved sensitivity, *J. Am. Chem. Soc. 114*, 10663–10665.

Kocur, M. (1986) in *Bergey's manual of systematic bacteriology*, vol. 2 (Sneath, P. H. A., ed.) pp. 1004–1008, Williams and Wilkins, Baltimore MD.

Krueger, P. J. & Mettee, H. D. (1964) Spectroscopic studies of alcohols. III Fundamental OH stretching bands of 2,2-di- and 2,2,2-tri-haloethanols, *Can. J. Chem. 42*, 340–346.

Maeji, N. J., Bray, A. M., Valerio, R. M. & Wang, W. (1995) Larger scale multipin peptide synthesis, *Peptide Res. 8*, 33–38.

Marion, D. & Wüthrich, K. (1983) Application of phase sensitive two-dimensional correlated spectroscopy (COSY) for measurements of ^{1}H-^{1}H spin-spin coupling constants in proteins, *Biochem. Biophys. Res. Commun. 113*, 967–974.

Marion, D., Zasloff, M. & Bax, A. (1988) A two-dimensional NMR study of the antimicrobial peptide magainin 2, *FEBS Lett. 227*, 21–26.

Merutka, G., Dyson, H. J. & Wright, P. E. (1995) 'Random coil' ^{1}H chemical shifts obtained as a function of temperature and trifluoroethanol concentration for the peptide series GGXGG, *J. Biomol. NMR 5*, 14–24.

Pastore, A. & Saudek, V. (1990) The relationship between chemical shift and secondary structure, *J. Magn. Reson. 90*, 165–176.

Presta, L. G. & Rose, G. D. (1988) Helix signals in proteins, *Science 240*, 1632–1641.

Ramamoorthy, A., Marassi, F. M., Zasloff, M. & Opella, S. J. (1995) Three-dimensional solid-state NMR spectroscopy of a peptide oriented in membrane bilayers, *J. Biomol. NMR 6*, 329–334.

Rance, M., Sørensen, O. W., Bodenhausen, G., Wagner, G., Ernst, R. R. & Wüthrich, K. (1983) Improved spectral resolution in COSY ^{1}H-NMR spectra of proteins via double quantum filtering, *Biochem. Biophys. Res. Commun. 117*, 479–485.

Richardson, J. S. & Richardson, D. C. (1988) Amino acid preferences for specific locations at the ends of α helices, *Science 240*, 1648–1652.

Shai, Y. (1995) Molecular recognition between membrane-spanning polypeptides, *Trends Biochem. Sci. 20*, 460–464.

Sönnichsen, F. D., Van Eyk, J. E., Hodges, R. S. & Sykes, B. D. (1992) Effect of trifluoroethanol on protein secondary structure: an NMR and CD study using a synthetic actin peptide, *Biochemistry 31*, 8790–8798.

Steinborner, S. T., Waugh, R. J., Bowie, J. H., Wallace, J. C., Tyler, M. J. & Ramsay, S. L. (1997) New caerin antibacterial peptides from the skin glands of the tree frog *Litoria xanthomera*, *J. Peptide Sci. 3*, 181–185.

Stone, D. J. M., Bowie, J. H., Tyler, M. J. & Wallace, J. C. (1992a) The structure of caerin 1.1, a novel peptide from Australian tree frogs, *J. Chem. Soc. Chem. Commun.*, 1224–1225.

Stone, D. J. M., Waugh, R. J., Bowie, J. H., Wallace, J. C. & Tyler, M. J. (1992b) Peptides from Australian frogs. Structures of the caerins and caeridin 1 from *Litoria splendida*, *J. Chem. Soc. Perkin Trans. 1*, 3173–3178.

Stone, D. J. M., Waugh, R. J., Bowie, J. H., Wallace, J. C. & Tyler, J. C. (1993) Peptides from Australian frogs. The structures of the caerins from *Litoria caerulea*, *J. Chem. Res. 138*, 910–936.

Storrs, R. W., Truckses, D. & Wemmer, D. E. (1992) Helix propagation in trifluoroethanol solutions, *Biopolymers 32*, 1695–1702.

Waugh, R. J., Stone, D. J. M., Bowie, J. H., Wallace, J. C. & Tyler, M. J. (1993) Peptides from Australian frogs. The structures of the caerins and caeridins from *Litoria gilleni*, *J. Chem. Res. 139*, 937–961.

Waugh, R. J., Steinborner, S. T., Bowie, J. H., Wallace, J. C., Tyler, M. J., Hu, P. & Gross, M. L. (1995) Two isomeric α and β aspartyl dodecapeptides and their cyclic amino succinyl analogue from the Australian green tree frog *Litoria gilleni*, *Aust. J. Chem. 48*, 1981–1987.

Wishart, D. S., Sykes, B. D. & Richards, F. M. (1991) Relationship between nuclear magnetic resonance chemical shift and protein secondary structure, *J. Mol. Biol. 222*, 311–333.

Wishart, D. S., Bigam, C. G., Holm, A., Hodges, R. S. & Sykes, B. D. (1995) ^{1}H, ^{13}C and ^{15}N random coil NMR chemical shifts of the common amino acids. I. Investigations of nearest-neighbor effects, *J. Biomol. NMR 5*, 67–81.

Woolfson, D. N. & Williams, D. H. (1990) The influence of proline residues on α-helical structure, *FEBS Lett. 277*, 185–188.

Wüthrich, K. (1986) *NMR of proteins and nucleic acids*, Wiley, New York.

Wüthrich, K., Billeter, M. & Braun, W. (1983) Pseudo-structures for the 20 common amino acids for use in studies of protein conformations by measurements of intramolecular proton-proton distance constraints with nuclear magnetic resonance, *J. Mol. Biol. 169*, 949–961.

Yi, G.-S., Park, C. B., Kim, S. C. & Cheong, C. (1996) Solution structure of an antimicrobial peptide buforin II, *FEBS Lett. 398*, 87–90.

Zuiderweg, E. R. P., Boelens, R. & Kaptein, R. (1985) Stereospecific assignments of ^{1}H-NMR methyl lines and conformation of valyl residues in the lac repressor headpiece, *Biopolymers 24*, 601–611.